

CONTRIBUTIONS TO COLLAPSE PREDICTION OF STEEL MOMENT FRAMES THROUGH RECENT EARTHQUAKE SIMULATOR COLLAPSE TESTS

Dimitrios G. Lignos¹, Helmut Krawinkler² and Andrew S. Whittaker³

ABSTRACT

This paper identifies contributions to collapse prediction of deteriorating structural systems under seismic excitations using the results of recent earthquake-simulator tests of two scale models of a four-story steel moment frame. The two model frames were tested at the NEES facility at the University at Buffalo. We conclude that the impact of second-order ($P-\Delta$) effects on sidesway instability of deteriorating structural systems can be quantified. Force distributions and overturning moments along the height of the model frames can be adequately predicted by simple analytical models provided that deterioration modeling of components is accurately simulated in the analytical predictions.

INTRODUCTION

Collapse assessment of structural systems under earthquake excitations is of fundamental concern in performance-based earthquake engineering. This research project focused on sidesway instability, where a story or a number of stories displace laterally a sufficient distance so that dynamic instability occurs due to $P-\Delta$ effects, which are accelerated by component deterioration.

One of the primary obstacles to an improved understanding of collapse was the lack of physical experiments of steel structures through collapse. Matsumiya et al. (2004) and Nakashima et al. (2006) conducted a full scale quasi-static test of a three-story moment frame to near collapse to evaluate the effectiveness of non-deteriorating analytical models used to trace structural behavior at large deformations. They concluded that such models can accurately reproduce the cyclic response of the structure up to drift angles of 1/25. Rodgers and Mahin (2004, 2008) investigated both experimentally and analytically the effect of local fracture-induced phenomena in steel moment frames using a one-third scale two-story one bay steel moment frame and concluded that global frame response is more sensitive to the underlying causes of local fracture-induced phenomena associated with strength stiffness and hysteretic response changes due to fracture. More recently, Suita et al. (2008) and Yamada et al. (2009) conducted a full scale earthquake simulator test through collapse of a 4-story building at E-Defense. Analytical studies [Tada et al. (2008), Lignos et al. (2009)] demonstrated that only after incorporating component deterioration in the analysis could the response of the structure be predicted adequately.

To better understand the effects of $P-\Delta$, which are accelerated by component deterioration, on the collapse capacity of structural systems, we conducted an experimental and analytical investigation on sidesway collapse of steel moment frames using two 1:8 scale models of a 4-

¹ Dept. of Civil and Environmental Engineering, Stanford University; Stanford, CA

² Dept. of Civil and Environmental Engineering, Stanford University; Stanford, CA

³ Dept. of Civil and Environmental Engineering, The State University of New York, University at Buffalo, NY

story frame designed using current seismic provisions. The objectives of the research project were: (1) to provide realistic experimental data on frame performance near collapse; (2) to assess the effect of cumulative damage on the global response of the two steel model frames; (3) to provide information regarding force redistribution due to member plastification and quantify $P-\Delta$ effects through collapse, and (4) to validate our numerical capabilities to trace dynamic collapse with 2-dimensional analytical models that utilize empirical deteriorating component models. The focus of this paper is on absolute accelerations, story forces and member force redistributions due cumulative damage. Analytical collapse predictions based on incremental dynamic analysis and quantification of $P-\Delta$ effects through collapse are discussed in Lignos et al. (2009).

EARTHQUAKE SIMULATOR COLLAPSE TESTS

Two scale models of a 4-story prototype steel moment frame with reduced beam sections (RBS) designed per current US seismic provisions (AISC 2005, FEMA 350) were fabricated in Buffalo and tested on the earthquake simulator of the Network of Earthquake Engineering Simulation (NEES) facility at the State University of New York at Buffalo (SUNY). Detailed information on the prototype can be found in Lignos et al. (2008, 2009) and Lignos and Krawinkler (2009). The two nominally identical 1:8 model frames were similitude scaled based on rules that are summarized by Moncarz and Krawinkler (1981). The scale of the model frame was dictated by the overturning capacity of the earthquake simulator at SUNY. The total simulated weight was about 40 kips. The concept was to conduct a test of the scaled moment resisting frame together with a mass simulator that carried the inertia and $P-\Delta$ forces. Figure 1 shows the model frame together with its leaning column (noted as mass simulator).

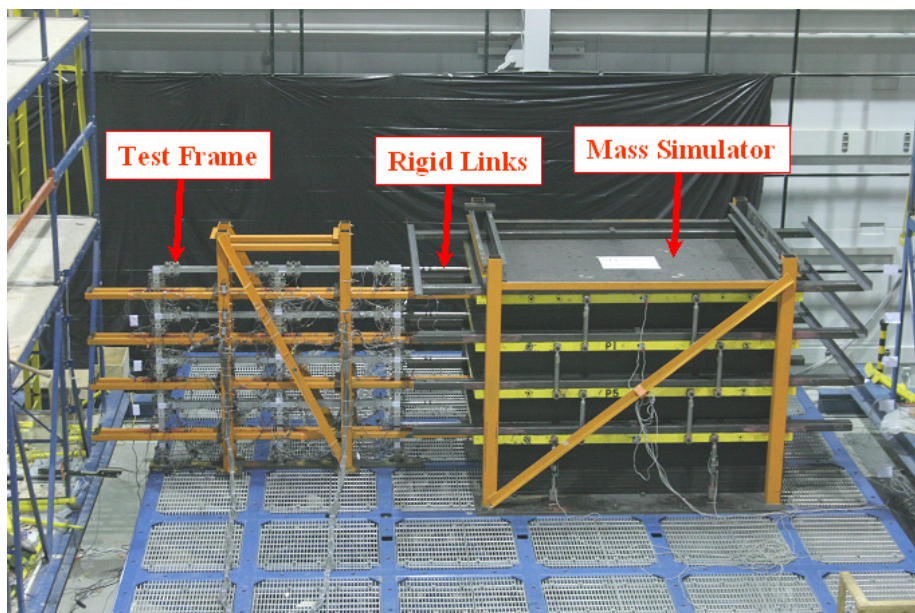


Fig. 1. Test setup on the NEES earthquake simulator

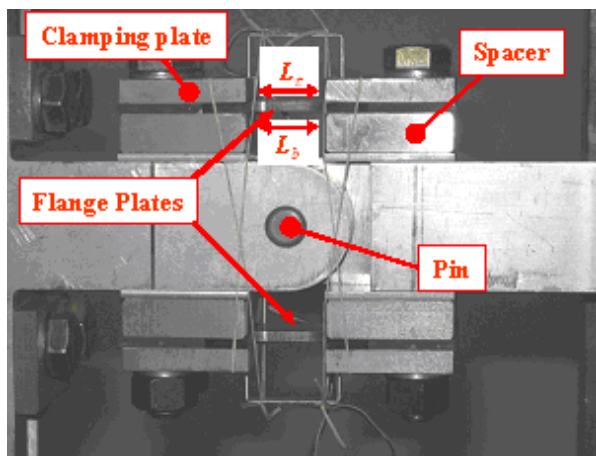
The two substructures were connected with axially “rigid” horizontal links also marked in Figure 1. These links were acting as load cells to measure forces due inertia and $P-\Delta$ effects from the mass simulator to the model frame. Both substructures were supported laterally with a bracing system since the intent was to conduct a unidirectional test. Details regarding instrumentation

(more than 300 channels), planning design and erection of the test setup shown in Figure 1 can be found in Lignos and Krawinkler (2009). This data set is available through NEES central repository (<https://central.nees.org/?projid=84&action=DisplayProjectMain>).

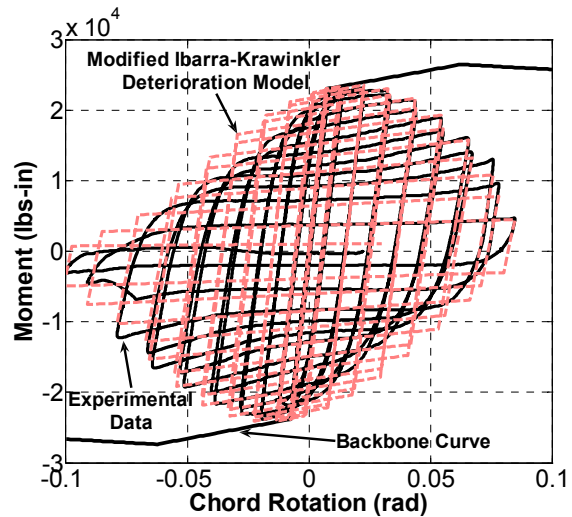
Test Frame and Modeling of Component Deterioration

The 1:8 scale model shown in Figure 1, consists of elastic elements (beams and columns) that are tuned such that the scaled lateral stiffness of the model frame matched the lateral stiffness of the prototype frame. To force inelastic deformation into discrete locations on the frame, plastic hinge elements were inserted at the ends of the beams and columns in the frame. The plastic hinge element shown in Figure 2a consists of two A572 steel flange plates to establish the moment capacity of the connection, a pin inserted in the center of the plastic hinge element to transmit shear force and four sets of clamp and spacer plates that controlled the deterioration characteristics of the hinge. The final geometry of all the plastic hinge elements was based on a component test program of 50 specimens conducted at Stanford University (Lignos and Krawinkler, 2009). The basic dimensions of the plastic hinge element shown in Figure 2 were varied to match targeted deterioration characteristics of prototype RBS connections.

The plastic hinge elements typically fractured at about 8% chord rotation when subjected to symmetric loading histories. Similar fracture chord rotations values have been reported for full-scale RBS connections [Ricles et al. 2004, Uang et al. 2000]. Due to the lack of a web in the plastic hinge element (1) web local buckling could not be simulated in the model frame and (2) the hysteretic response of the elements becomes slightly pinched at large deformations (see Figure 2b). Component degradation was evident in the plastic hinge elements and was modeled with a modified version of the Ibarra-Krawinkler empirical deterioration model (Ibarra and Krawinkler, 2005, Lignos and Krawinkler, 2009). This model is a concentrated plasticity spring that incorporates hysteretic rules capable to simulate important component deteriorating modes. A comparison between symmetric cyclic responses of a plastic hinge element with the calibrated IK model is shown in Figure 2b.



(a) plastic hinge element



(b) calibrated hysteretic response

Fig. 2. Typical plastic hinge element and its hysteretic response under symmetric loading protocol

TESTING PROGRAM AND ASSESSMENT OF RESULTS NEAR COLLAPSE

Each frame was subjected to four series of tests on the earthquake simulator as summarized in Table 1 together with the testing phase notation. The last series (CLEF: “Final” Collapse Level Earthquake) was conducted because both frames did not collapse as expected during the Collapse Level Earthquake (CLE) series as suggested by pre-test predictions. Since the focus is on behavior near collapse, the emphasis in the following discussion is placed on the last two series (CLE and CLEF). A detailed assessment of all tests is presented in Lignos and Krawinkler, (2009). Frame #1 was subjected to the Northridge 1994 Canoga Park record with accelerations scaled incrementally. Figure 3a shows the roof drift history of Frame#1 together with analytical predictions based on the post-test numerical model discussed in Lignos and Krawinkler, (2009). After drifting in one direction (ratcheting) Frame #1 collapsed during the first cycle of the CLEF with a complete 3-story collapse mechanism (see Figure 3a). For Frame #2 during the Maximum Considered Earthquake (MCE) the 150% Chile 1985 Llole record was used since the intent was to investigate the effect of cumulative damage on the collapse capacity of the test frame. Due to unsuccessful reproduction of the input ground motion residual deformations of Frame #2 after MCE were the same as after DLE. During CLEF Frame #2 finally collapsed in the opposite direction compared to Frame #1 but with the same collapse mechanism. Numerical simulations of roof drift histories for CLE and CLEF phase of Frame #2 are presented in Figure 3b and are in a good agreement with experimental results.

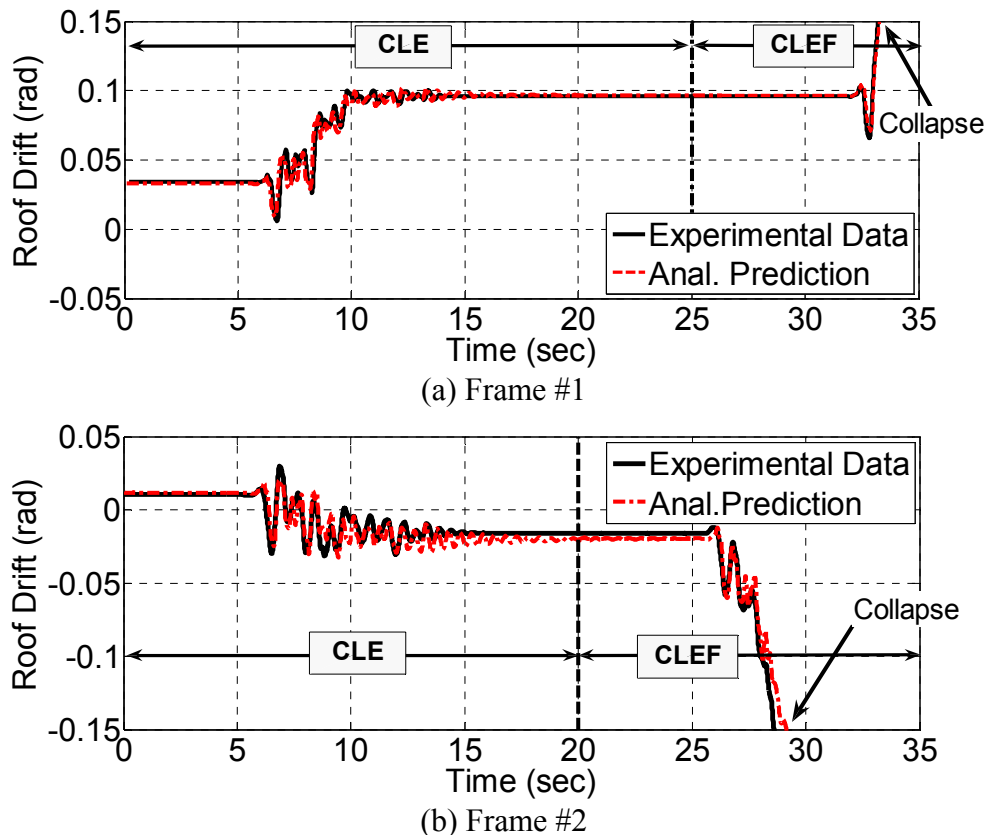


Fig. 3. Roof drift histories for both frames during CLE and CLEF testing phases together with analytical predictions

Table 1. Testing phases during earthquake simulator collapse tests for both frames

Testing Phases		Frame #1		Frame #2	
Phase	Notation	Ground Motion Station	Scale Factor	Ground Motion Station	Scale Factor
Service Level Event	SLE	Canoga Park	40%	Canoga Park	40%
Design Level Event	DLE	Canoga Park	100%	Canoga Park	100%
Maximum Considered Event	MCE	Canoga Park	150%	Llolleo	150%
Collapse Level Event	CLE	Canoga Park	190%	Canoga Park	220%
"Final" Collapse Level Event	CLEF	Canoga Park	220%	Canoga Park	220%

Acceleration Response

Recorded absolute accelerations are important to establish floor inertia forces. Three accelerometers per floor were installed: two per floor on the mass simulator, $a_{M,avg.}$, and one at the center of the left beams of the test frames, a_F . Acceleration measurements from the mass simulator $a_{M,avg.}$ were used to compute the inertial story forces by multiplying $a_{M,avg.}$ with the individual story mass. Figure 4 enables a comparison of peak absolute accelerations per floor for CLE shaking together with peak absolute accelerations based on analytical predictions. As indicated from the same figure the analytical predictions of peak absolute accelerations follow the same trends as the recorded accelerations but they are slightly overestimated compared to the experimental data.

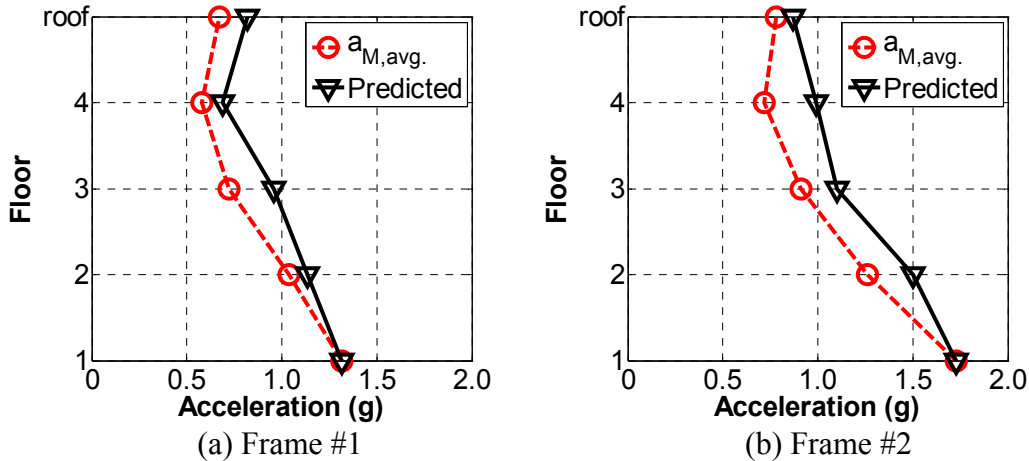


Fig. 4. Peak absolute acceleration along the height of both frames during CLE

Story Shear Forces and Overturning Moments

The test setup with the near-weightless scale model and the mass simulator allowed us to compute the inertia-based story shear forces, V_i^a , as summations of the product of absolute accelerations and floor masses. Load cells were installed in the links between the test frame and the mass simulator and these load cells were used to compute the story shear forces generated by inertia plus $P-\Delta$ effects, V_i^L , noted as effective forces. Figure 5 shows the normalized “effective” story shear forces with respect to gravity W along the height of Frame #1 for a time window of CLEF prior to collapse ($t_{collapse} \sim 7.2$ sec). The roof drift history is also presented in the figure.

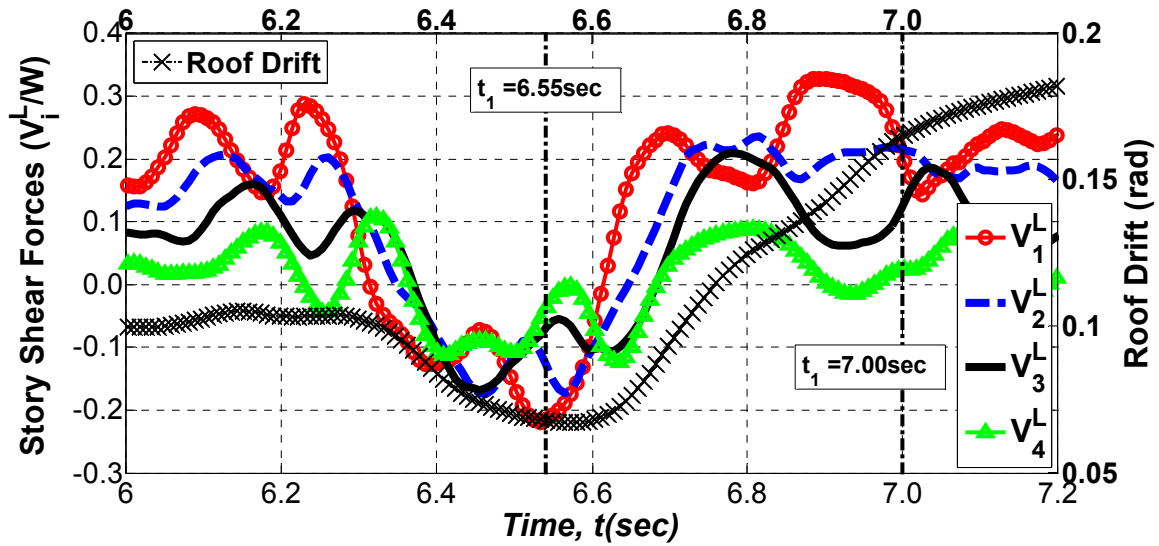


Fig. 5. Effective story shear force histories for Frame #1, CLEF

As seen from Figure 5, the story shear force maxima are not well synchronized and indicate that higher mode responses can be important in frames that are assumed to be first-mode dominated. The effective story shear forces develop their maximum values at roof displacements smaller than the maximum displacements because large displacements cause large $P-\Delta$ effects, which in turn reduce the inertial forces that can be resisted in the inelastic range (Aiken et al. 1993). Figure 6 shows normalized inertia-based and effective story shear forces along the height of Frame #1 at selected times during CLEF together with analytically predicted story shear forces. The difference between V_i^L and V_i^a in Figure 6 is attributed to $P-\Delta$ effects and can be quantified with a simple $P \cdot \delta/h$ term [Lignos et al. 2009].

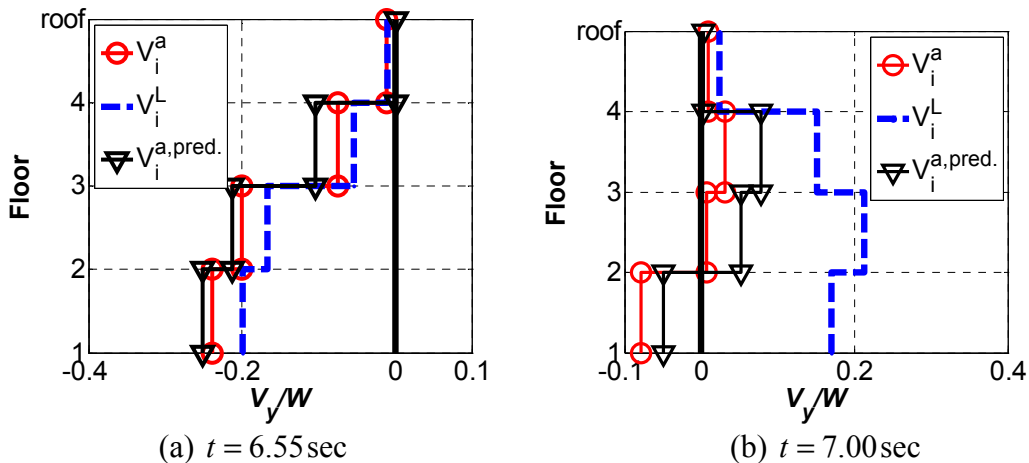


Fig. 6. Story shear force distributions along the height of Frame #1 during CLEF for selected times together with analytical predictions

The overturning moment histories (OTM) at the base of both frames near collapse are presented in Figure 7 for both inertia-based OTM_{Base}^a and effective OTM_{Base}^L . As with story shear forces the difference between the two measurements is attributed to $P-\Delta$ effects. From the same figures it

can be seen that the correlation between analytically predicted and measured OTMs is good, even at large deformations.

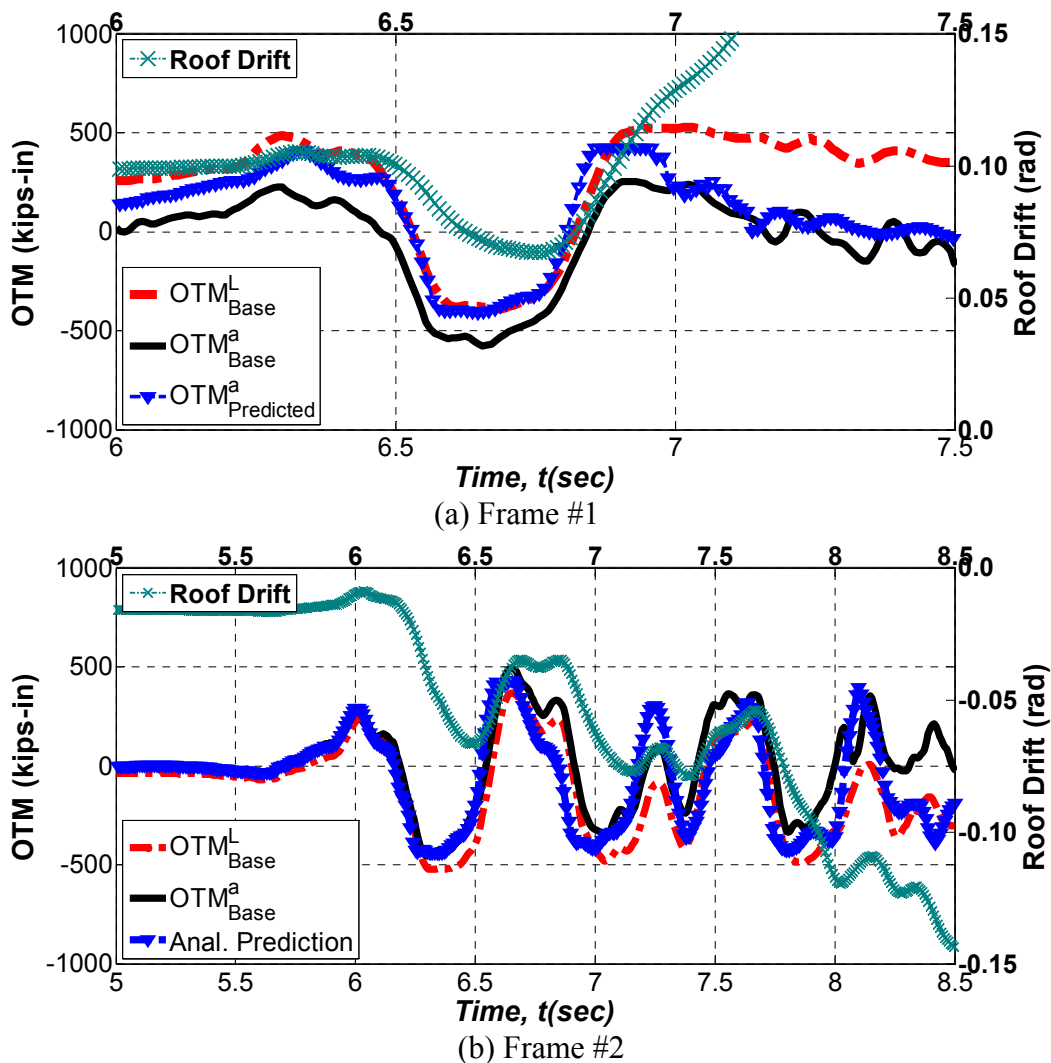
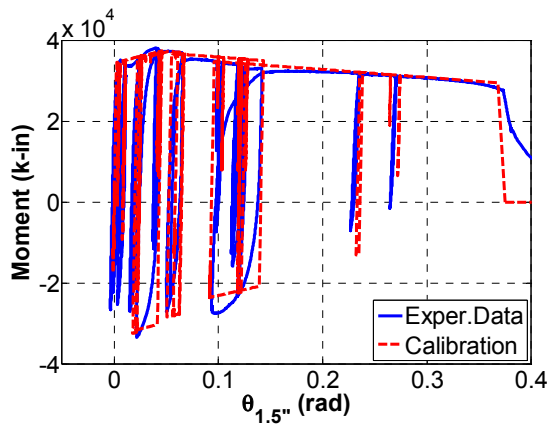


Fig. 7. Overturning moment history at base for both frames, CLEF

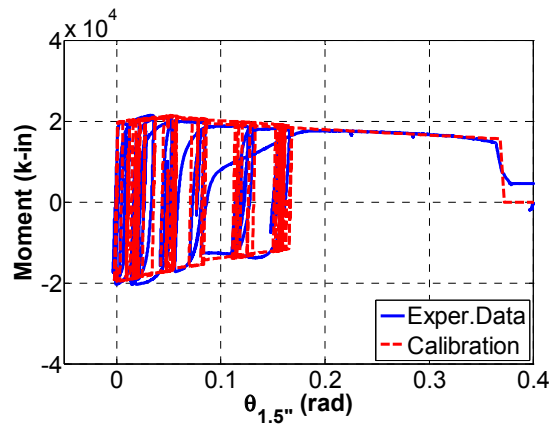
Moment Redistribution of Components Near Collapse

Based on the component tests, Lignos and Krawinkler, (2009) showed that the strain–moment calibrations provide reliable moment measurements in the elastic range. For the plastic hinge elements that responded nonlinearly, we obtained moment-rotation diagrams from component experiments by subjecting plastic hinge elements identical to the ones from Frame #1 to the rotation histories recorded in the earthquake simulator tests.

Figure 8 shows the moment-rotation diagram for an exterior column base and a first floor beam for Frame #1. The results of analysis using the calibrated IK deterioration model are also superimposed in the same figure. Note that the analytical model is able to simulate fracture at large rotations ($\theta_{1.5''} \sim 0.37rad$). As seen in this figure both elements that are part of the collapse mechanism deteriorate in strength at rotations $\theta_{1.5''}$ (rotation over 1.5" length) of the order of 4%.



(a) Exterior column at base



(b) first floor beam at exterior corner

Fig. 8. Moment-rotation histories for selected plastic hinge elements of Frame #1

Figure 9 shows the moment equilibrium at selected locations at instants in time during the CLE and CLEF shaking. For the plastic hinge elements that behaved elastically during the tests (column at top of first story and bottom second story) moments were calculated based on an equivalent modulus and using the strain measurements from the flange plates (see Lignos and Krawinkler, 2009). The moment values that are shown in Figure 9 have been extrapolated from the plastic hinge elements to the centerline of the exterior joint. The data of Figure 9 makes it clear that the moment gradient in the column can vary significantly based on the loading history that the column ends experience.

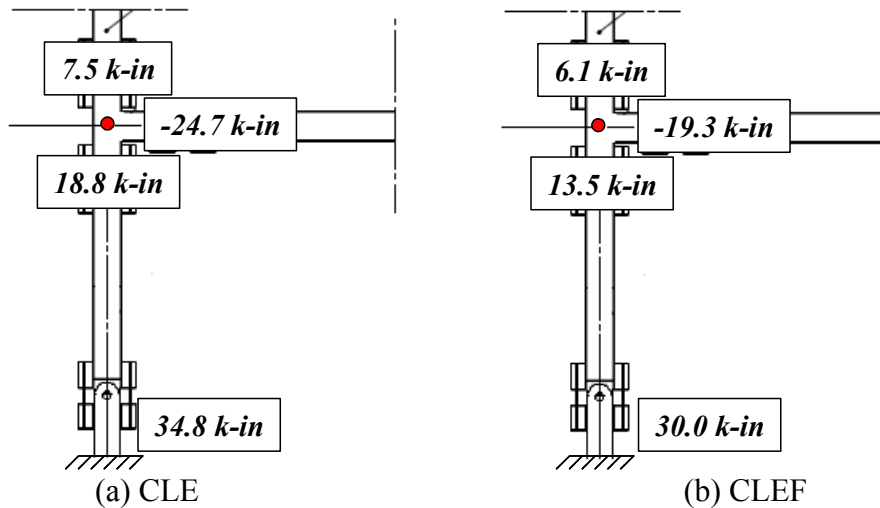


Fig. 9. Moment distribution of exterior subassembly at first story during CLE and CLEF

SUMMARY AND CONCLUSIONS

This paper summarizes research on prediction of sidesway collapse of steel frame structures under earthquake excitations based on recent earthquake simulator tests of two scale models tested through collapse. The two nominally identical test frames represent a 1:8 scale model of a prototype 4-story steel moment frame with reduced beam sections designed based on current seismic provisions. The two nominally identical frames were subjected to four scheduled levels of intensity through collapse. Both frames collapsed with the same complete three story mechanism. Both earthquake simulator collapse test series demonstrated the value of the comprehensive set of collected data and facilitated the study of phenomena that otherwise could be evaluated only from results of numerical investigations. This data set is available through NEES central repository (<https://central.nees.org/?projid=84&action=DisplayProjectMain>). The focus of this paper was on acceleration responses, shear force and overturning moments and moment redistribution of components near collapse. Based on the experimental data and analytical predictions the main conclusions are:

- The difference between inertia-based and effective story shear forces is attributed to $P-\Delta$ effects and can be quantified with a simplified $P \cdot \delta/h$ term.
- The maxima of story shear forces and overturning moments are not well synchronized indicating that even for first mode dominated structures, the effects of higher modes on distribution of story shear force is important.
- Critical components that are part of the collapse mechanism of frame structures deteriorate at large deformations, and due to plastification of their moment gradient can vary significantly.
- Phenomenological models that simulate accurately component deterioration under cyclic loading can be used with numerical tools to accurately predict global response near collapse.

ACKNOWLEDGEMENTS

This study is based on work supported by the United States National Science Foundation (NSF) under Grant No. [CMS-0421551](#) within the George E. Brown, Jr. Network for Earthquake Engineering Simulation Consortium Operations. The financial support of NSF is gratefully acknowledged. The authors also thank REU students, Mathew Alborn, Melissa Norlund and Kar Him Chiu for their invaluable assistance during the earthquake simulator collapse test series. The successful execution of earthquake-simulator testing program would not have been possible without the assistance and guidance of the laboratory technical staff at the NEES Equipment Site at the University at Buffalo. Any opinions, findings, and conclusions or recommendations expressed in this paper are those of the authors and do not necessarily reflect the views of NSF.

REFERENCES

- Aiken, I. D., Nims, K., Whittaker, A. S., Kelly, J. M. (1993). Testing of passive energy dissipation systems. *Earthquake Spectra*, **9** (3): 335-370
- AISC. 2005. Seismic provisions for structural steel buildings, including supplement No. 1. *American Institute of Steel Construction, Inc. Chicago, Illinois, 2005.*
- FEMA-350. 2000. Recommended seismic design criteria for new steel moment frame buildings. *Report No. FEMA 350, Federal Emergency Management Agency, Washington, D.C., 2000.*
- Ibarra, L. F., Krawinkler, H. 2005. *Global collapse of frame structures under seismic excitations.* PEER Report 2005/06, Pacific Earthquake Engineering Research Center, Berkeley, Calif.
- Lignos, D. G., Krawinkler, H., Whittaker, A. 2008. Shaking table collapse tests of a 4-story steel moment frame. *Proceedings, 14th World Conference on Earthquake Engineering 2008, October 12-17, 2008, China.*
- Lignos, D. G. Krawinkler, H. 2009. Sidesway collapse of deteriorating structural systems under seismic excitations. *Report No. TR 172, John A. Blume Earthquake Engineering Center, Department of Civil and Environmental Engineering, Stanford University, CA.*
- Lignos, D. G., Krawinkler, H., Whittaker, H. 2009. Prediction and validation of sidesway collapse of two scale models of a 4-story steel moment frame. *Earthquake Engineering & Structural Dynamics* (under review).
- Matsumiya, T., Suita K., Chusilp, P., Nakashima, M. 2004. Full-scale test of three-story steel moment frames for examination of extremely large deformation and collapse behavior. *Proceedings, 13th World Conference on Earthquake Engineering, Vancouver, Paper No. 3471, 1–6 August 2004.*
- Moncarz, P.D., Krawinkler, H. 1981. Theory and application of experimental model analysis in earthquake engineering. *Report No. TR 50, John A. Blume Earthquake Engineering Center, Department of Civil and Environmental Engineering, Stanford University, CA.*
- Nakashima, M., Matsumiya, T., Suta, K., Liu, D. 2008. Test on full-scale three-storey steel moment frame and assessment of ability of numerical simulation to trace cyclic inelastic response. *Earthquake Engineering & Structural Dynamics* **35**:3–19.
- Rodgers, J. E., and Mahin, S. A. 2004. *Effects of connection hysteretic degradation on the seismic behavior of steel moment-resisting frames.* PEER Report 2003/13. Pacific Earthquake Engineering Research Center, Berkeley, Calif.
- Rodgers, J. E., and Mahin, S. A. 2008. Local fracture-induced phenomena in steel moment frames. *Earthquake Engineering & Structural Dynamics* **38**:135–155.
- Suita, K., Yamada, S., Tada, M., Kasai, K., Matsuoka, Y. Shimada, Y. 2008. Collapse experiment on 4-story steel moment frame: Part 2 detail of collapse behavior. *Proceedings 14th World Conf. on Earthquake Engineering, Beijing, China.*
- Uang, C.M., Yu, K., Gilton, C. 2000. *Cyclic response of RBS moment connections: Loading sequence and lateral bracing effects,* SSRP Report 99/13. Department of Structural Engineering, University of California San Diego, Calif.
- Yamada, S., Kasai, K., Shimada, Y., Suita, K., Tada, M., Matsuoka, Y. 2009. Full scale collapse experiment on 4-story steel moment frame: part 1 outline of the experiment. *Proceedings 6th International Conference on Behavior of Steel Structures in Seismic Areas, STESSA 2009, Philadelphia, Pennsylvania, USA.*